Adaptive finite element analysis for damage detection of Non–uniform Euler–Bernoulli beams with multiple cracks based on natural frequencies

ABSTRACT

Purpose

In this study, an adaptive finite element method (FEM) is developed for structural eigenproblems of cracked Euler–Bernoulli beams via the superconvergent patch recovery displacement technique. This research comprises the numerical algorithm and experimental results for free vibration problems (forward eigenproblems) and damage detection problems (inverse eigenproblems).

Design/methodology/approach

The weakened properties analogy is used to describe cracks in this model. The adaptive strategy proposed in this paper provides accurate, efficient, and reliable eigensolutions of frequency and mode (i.e. eigenpairs as eigenvalue and eigenfunction) for Euler–Bernoulli beams with multiple cracks. Based on the frequency measurement method for damage detection, utilizing the difference between the actual and computed frequencies of cracked beams, the inverse eigenproblems are solved iteratively for identifying the residuals of locations and sizes of the cracks by the Newton–Raphson iteration technique. In the crack detection, the estimated residuals are added to obtain reliable results, which is an iteration process that will be expedited by more accurate frequency solutions based on the proposed method for free vibration problems.

Findings

Numerical results are presented for free vibration problems and damage detection problems of representative non-uniform and geometrically stepped Euler–Bernoulli beams with multiple cracks to demonstrate the effectiveness, efficiency, accuracy and reliability of the proposed method.

Originality/value

The proposed combination of methodologies described in the paper, leads to a very powerful approach for free vibration and damage detection of beams with cracks, introducing the mesh refinement, that can be extended to deal with the damage detection of frame structures.

KEYWORDS: Adaptive finite element method, Beam with multiple cracks, Damage detection, Free vibration, Forward eigenproblems, Inverse eigenproblems

1. INTRODUCTION

Free vibration and damage detection problems for frame structures are widespread in engineering practice. In one of the special cases, the beam members contain multiple cracks, and the existence of these cracks changes the mechanical properties of the entire structure, thereby affecting its safety and applicability. Exploration of the dynamic characteristics and identification of crack locations and sizes for frame structures with multiple cracks, as shown in Figure 1, effectively guarantees the safety of the structures throughout their life cycles. Based on the dynamic characteristics of a cracked structure, there are well-developed damage detection methods (Wang *et al*., 1997; Hassiotis and Jeong, 1993). Damage detection methodologies based on actual measured frequencies are practical and effective for evaluating frame structures with multiple cracks (Pawar, P.M. and Ganguli, R., 2003; Zacharias *et al*., 2004; Yan *et al*., 2007) .

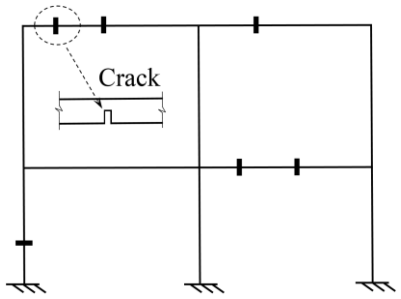

Figure 1. Frame structure with multiple cracks.

As shown in Figure 2, the free vibration of a beam with cracks is a forward eigenproblem that involves solving for the frequencies and modes based on knowledge of the material properties. Correspondingly, damage detection is an inverse eigenproblem that involves solving for the material properties (i.e. cracks) and modes based on knowledge of the actual frequencies (Farrar *et al*., 2001). The present paper addresses both forward eigenproblems and inverse eigenproblems.

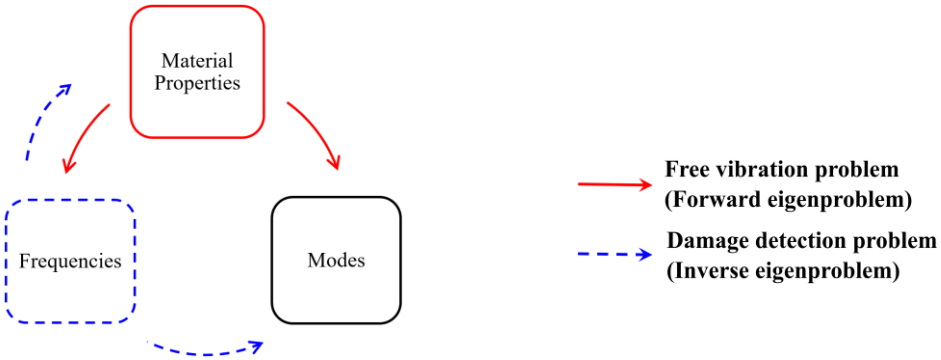

Figure 2. Free vibration problem (forward eigenproblem) and damage detection problem (inverse eigenproblem) of a beam with multiple cracks

In recent years, several other methods have been proposed that are dedicated to free vibration

forward eigenproblems. Methods for free vibration of uncracked beams are well developed: e.g. Euler–Bernoulli beams and shear-flexible arches with various cross-section depths and various types of supports (Wang *et al*., 2015; Kaveh and Dadfar, 2007; Litewka and Rakowski, 2001); consequently, the corresponding forward eigenproblems for cracked beams naturally became the next research target. Labib et al. (2014) used the exact dynamic method and the Wittrick–Williams algorithm to solve the free vibration of beams and frames with multiple cracks; the method is applied effectively for uniform beams. Nandwana and Maiti (1997) and Chaudhari and Maiti (2000) used semi-analytical methods for solving free vibration problems for cracked beams. To the best of the authors' knowledge, SLEUTH (Greenberg and Marletta, 1997) is the only code that specifically solves beam members based on Euler–Bernoulli beam theory in the challenging form of a regular fourth-order eigenproblem. SLEUTH uses piecewise constant approximations of the variable coefficients in fourth-order eigenproblems with shooting methods used to locate eigenvalues. Unfortunately, this code does not impose error control on the eigenfunctions; hence, it cannot serve as a complete eigensolver. Caddemi and Morassi (2013) used Heaviside and Dirac's delta distribution functions to solve vibration problems of Euler–Bernoulli beam with multiple cracks. Caddemi and Caliò (2014) proposed an exact procedure for the reconstruction of multiple instances of concentrated damage on a straight beam. Hsu (2005) formulated the eigenvalue problems for clamp-free and double-hinged Euler–Bernoulli beams with elastic foundations, a single edge crack, axial loading, and excitation force by using the differential quadrature method. Rizos et al. (1990) simulated cracks in beam members as springs with rotational stiffness and used the actual frequencies to identify damage; their results were in good agreement with the experimental analysis, so the crack model has widely been used in subsequent finite element (FE) analyses. Chinchalkar (2001) also used the approximation of a spring with rotational stiffness within the conventional finite element method (FEM) to solve the free vibration problem for cracked wedges and two-segment beams. Lee (2009) used the conventional FEM to analyse cantilever beams with two and three cracks. Therefore, it is necessary to reliably solve problems for the accurate frequencies and modes of non-uniform beams with multiple cracks. Furthermore, damage detection can be well developed based on these dynamic solutions. The above FE methods are generally not adaptivity-oriented and lack aspects required in an adaptive package.

To improve the validity and reliability of conventional FEM for solving free vibration problems, adaptive FEM has been proposed. Superconvergent patch recovery (SPR) and the corresponding

adaptive technique originally proposed by Zienkiewicz and Zhu (1992a, 1992b) have been applied to static and dynamic problems to estimate spatial discretisation errors and to improve the solution of stresses. For problems on the free vibration of beams and structures without cracks, Wiberg et al. (1999a, 1999b) presented an application of local and global updating methods to improve the natural frequencies and modes predicted by the FE solutions in free vibration analysis, in which the local updating was based upon the superconvergent patch recovery displacements technique. The adaptive mesh refinement technique of FEM has been utilized to establish a three-dimensional model for rock stability analysis (Wang *et al*., 2017a, 2017b). Furthermore, adaptive FEM has been applied to successfully solve structure eigenvalue problems: e.g. buckling problems for non-uniform Euler–Bernoulli beam members (Yuan *et al*., 2013) and free vibration problems for two-dimensional structures (Yuan *et al*., 2014).

Considering the practical and theoretical importance of these problems, the crack detection problem has been extensively investigated as an inverse eigenproblem in structures, and many methods have been proposed to solve this problem, as have been comprehensively summarized in the summary of Dimarogonas (1996). Most fundamental studies concerning crack detection in a beam dealt with cases of single crack. The frequency contour plot method has been one of the most favoured tools to identify a single crack by using the lowest three natural frequencies obtained via a frequency measurement method (Moezi *et al*., 2015; Guan and Karbhari, 2008). Owolabi et al. (2003) proposed that the location and size of a crack could be identified by finding changes in frequencies and amplitudes of frequency response functions. A beam with multiple cracks was modelled as a massless rotational spring or other models based on the Euler–Bernoulli theory, and this scheme was subsequently adopted for crack detection in stepped beams (Maghsoodi, *et al*., 2013; Al-Said, 2007, 2008). In most studies, the crack was assumed to be open and normal to the beam surface. Morassi (2001) studied crack detection problems involving an inclined- edge-type crack or a crack beneath the beam surface. Lele and Maiti (2002) and Nikolakopoulos et al. (1997) extended the frequency contour plot method to the crack detection in beams based on the Timoshenko beam theory and in-plane frame, respectively. In many cases, the three curves of the frequency contour plot unfortunately did not intersect because of the inaccuracy of modelling results as compared to measured results, and the zero-setting procedure was recommended for such cases (Maghsoodi, *et al*., 2013; Al-Said, 2007, 2008; Morassi, 2001; Morassi, 2001). Narkis (1994) showed that, if a crack is very small, the only information required

for crack detection is the variation of the first two natural frequencies due to a crack. Dado (1997) presented a direct mathematical model to detect a crack in a beam, where the lowest two natural frequencies were required as input data. Hu and Liang (1993) introduced a technique to detect multiple cracks. The continuum damage model was used to identify the discretizing elements of a structure that contained the cracks, and the spring damage model was used to quantify the location and size of the discrete crack in each damaged element. Patil and Maiti (2003) presented a method that combined vibration modelling through the transfer matrix method and the approach proposed by Hu and Liang (1993). The detection of multiple cracks in beams was regarded as an optimization problem by Ruotolo and Surace (1997), who selected the combination of fundamental functions as the objective function and utilized a solution procedure employing generic algorithms. Shifrin and Ruotolo (1999) proposed that $n+2$ equations are sufficient to form the system determinant for a beam with n cracks. Labib et al. used the Wittrick-Williams algorithm and dynamic stiffness method to analyse the free vibration and detect the cracks of cracked structures (Labib *et al*., 2014, 2015), but their analytical method is only applicable to beams with uniform cross sections. Using the traditional FEM and cracks modelled as rotational springs, Chinchalkar (2001) determined crack location in beams using natural frequencies for cracked wedge and two- segment beams, on the other hand, in the similar approach, Lee et al. (2009) identified a cantilever beam with triple as well as double cracks. The above FE methods are generally not adaptivity oriented and lack the ingredients required in an adaptive package. Furthermore, the basic methodology for damage detection based on the dynamic solutions is well developed; on the other hand, it is necessary to solve the problem of acquiring reliable and accurate frequencies and modes for non-uniform beams with multiple cracks.

This paper initially introduced an adaptive method based on the conventional FEM and the superconvergent patch recovery displacement technique for solving forward eigenproblems of beams with multiple cracks. The superconvergent computation technique is applied to calculate superconvergent solutions, which are henceforth referred to as superconvergent solutions, for eigenfunctions during the FE post-processing stage. These superconvergent solutions are then used as if they were exact solutions to estimate the errors in the FE solutions, which are used to guide mesh refinement. This yields a simple, efficient, reliable, and general adaptive FE procedure that can find sufficiently fine meshes to obtain FE solutions with the desired accuracy for the eigenvalues and eigenfunctions for beams with multiple cracks. Based on the solution dynamic

solutions of forward eigenproblems, the inverse eigenproblems could be solved smoothly. The objective of the present study is to present an adaptive FE algorithm and procedure based on the adaptive FE solutions of frequencies via the superconvergent computation technique and on the Newton–Raphson iteration technique to identify multiple cracks in a beam, which requires 2*n* natural frequencies to detect *n* cracks in a beam. In this paper, the presented procedure is applied to inverse eigenproblems of a beam with multiple cracks by utilizing the Newton–Raphson iteration technique to obtain damage information. Our simple, efficient, reliable, and generally adaptive FE procedure can find sufficiently fine meshes such that the obtained FE solutions satisfy the pre-specified error tolerance for both the locations and sizes of cracks in beams with multiple cracks.

2. ADAPTIVE APPROACH FOR DAMAGE DETECTION OF CRACKED BEAMS

2.1 Formulation and analogy of cracked beams

The goal of solving a regular fourth-order eigenproblem for a beam member based on Euler–Bernoulli beam theory is to find the frequencies ω and modes w of the fourth-order ordinary differential equation (ODE),

$$Lw \equiv (EI(x)w'')'' = \omega^2 m(x)w, \quad 0 < x < l, \tag{1}$$

subject to the default boundary conditions (BCs),

$$w(0) = 0, \quad w'(0) = 0, \quad w(l) = 0, \quad w'(l) = 0, \tag{2}$$

where $EI(x)$ is the member's flexural rigidity, E is the elastic modulus, $m(x)$ is the linear density, and l is the length of the beam. The symbol L used in Eq. (1) is the associated fourth-order self-adjoint operator. In the eigenproblem, the frequency and mode are the eigenvalue and eigenfunction, respectively, which together are known as an eigenpair.

Figure 3 demonstrates a geometric model of a beam with cracks. Here, parameters $\alpha = a/h$ and $\beta = s/l$ denote the normalized crack depth and location, respectively, where a and s are the absolute crack depth and location, and h is the height of the beam.

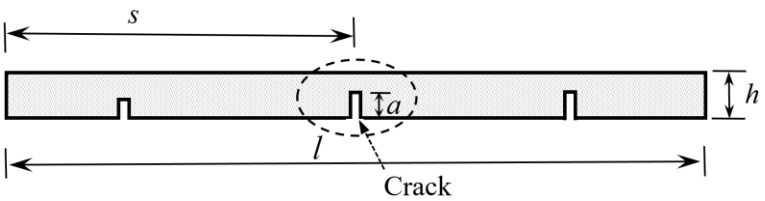

Figure 3. Beam with multiple cracks.

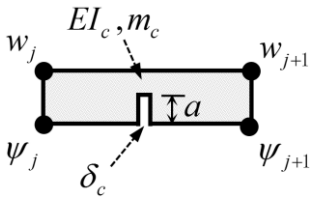

Figure 4. FE model with crack.

In the immediate region surrounding a single crack, the FE element containing the crack has

two nodes with four degrees of bending and rotational freedoms (w_j, ψ_j) and (w_{j+1}, ψ_{j+1}), as shown in Figure 4, where the narrow crack is described with a width δ_c set at $0.01 \times Tol$, where Tol is the pre-specified error tolerance for both frequencies and modes. Using the weakened properties analogy to reflect the presence of cracks, the flexural rigidity and density at the crack are reduced as the crack deepens:

$$EI_c = \frac{Ebh^3(1-\alpha)^3}{12} \tag{3a}$$

$$m_c = \overline{m}bh(1-\alpha) \tag{3b}$$

where EI_c and m_c are the flexural rigidity and linear density at crack c respectively; b is the width of the beam and $\overline{m}$ is the density.

2.2 Stop criterion

Suppose n cracks (α_i, β_i) $(i = 1,2,\mathrm{K}\,,n)$ are required and the pre-specified error tolerance for both the locations and sizes is Tol. The ultimate aim of the procedure presented here is to find FE solutions (α_i^h, β_i^h) $(i = 1,2,\mathrm{K}\,,n)$ on sufficiently fine meshes π such that

$$\alpha_i - \alpha_i^h < Tol \cdot (1+\alpha_i), \qquad i = 1,2,\mathrm{K}\,,n \tag{4a}$$

$$\beta_i - \beta_i^h < Tol \cdot (1+\beta_i), \qquad i = 1,2,\mathrm{K}\,,n \tag{4b}$$

Since the exact solutions (α_i, β_i) are not usually available, the proposed procedure uses the following stop criterion instead:

$$\omega_k^h - \omega_k < Tol \cdot (1+\omega_k), \qquad k = 1,2,\mathrm{K}\,,2n \tag{5}$$

where ω_k and ω_k^h are the actual and computed frequencies of cracked beams, respectively. The above stop criteria in absolute error estimation for eigensolutions in adaptive analysis show satisfying effect (Yuan *et al*., 2013; Yuan *et al*., 2014; Yuan *et al*., 2017).

In detail, as summarized in Table I, the ultimate aim of damage detection is to obtain the exact solution of the problems. Unfortunately, the exact solution cannot be obtained for major problems; consequently, no solution can be used as the stop criterion. Therefore, the proposed procedure uses the new stop criterion introduced in Eq. (5), which has been shown to be effective through some numerical results involving the examples in Section 7. According to the uniqueness theory of the solution, the errors of each crack location and size compared to the exact solution are consistent with the errors of each frequency compared to the actual frequency for the structure with cracks; therefore, the latter is used as the stopping criterion in the proposed method.

Table I. Ultimate aim and stop criterion.

Problem type	Ultimate aim	Stop criterion
Damage detection problem (Inverse eigenproblem)	☒ Errors of FE solutions of each crack location and size compared to the exact solution are less than *Tolerance*	☑ Errors of FE solution of each frequency compared to the actual frequency for a beam with cracks are less than *Tolerance*

2.3 Analysis strategy

The adaptive FEM algorithm contains the free vibration analysis and damage detection of a beam with cracks, which are the forward eigenproblem and inverse eigenproblem, respectively, as shown in Figure 5. The proposed method intends to combine the free vibration analysis and the Newton–Raphson iteration technique to solve the inverse eigenproblem through the following three-step adaptive strategy:

(1) Adaptive analysis. Under the current crack damage condition (the initial crack damage is provided by the user), the computed frequencies fully satisfy the pre-specified error tolerance by the adaptive FEM (forward eigenproblems), as described in Section 3.

(2) Newton–Raphson iteration. Utilizing the difference between computed frequencies and actual frequencies, the damage residuals of the computed and actual cracks are obtained by the Newton–Raphson iteration technique, as described in Section 4.

(3) Damage refinement. The crack locations and sizes are updated by the residuals of cracks damage to form the new crack damage condition. Then, the procedure returns to the first step (i.e., adaptive analysis) until all frequency errors satisfy the pre-specified error tolerance, as described in Section 5.

3. ADAPTIVE ANALYSIS

3.1 FE solution

Utilizing the conventional FEM, the element stiffness matrix $\mathbf{K}^e$ and mass matrix $\mathbf{M}^e$ are computed and assembled to form the global stiffness matrix $\mathbf{K}$ and mass matrix $\mathbf{M}$. The FE equation of a beam member based on Euler–Bernoulli beam theory can be derived as an eigenvalue equation in the following matrix form:

$$\mathbf{KD} = \omega^2 \mathbf{MD} \tag{6}$$

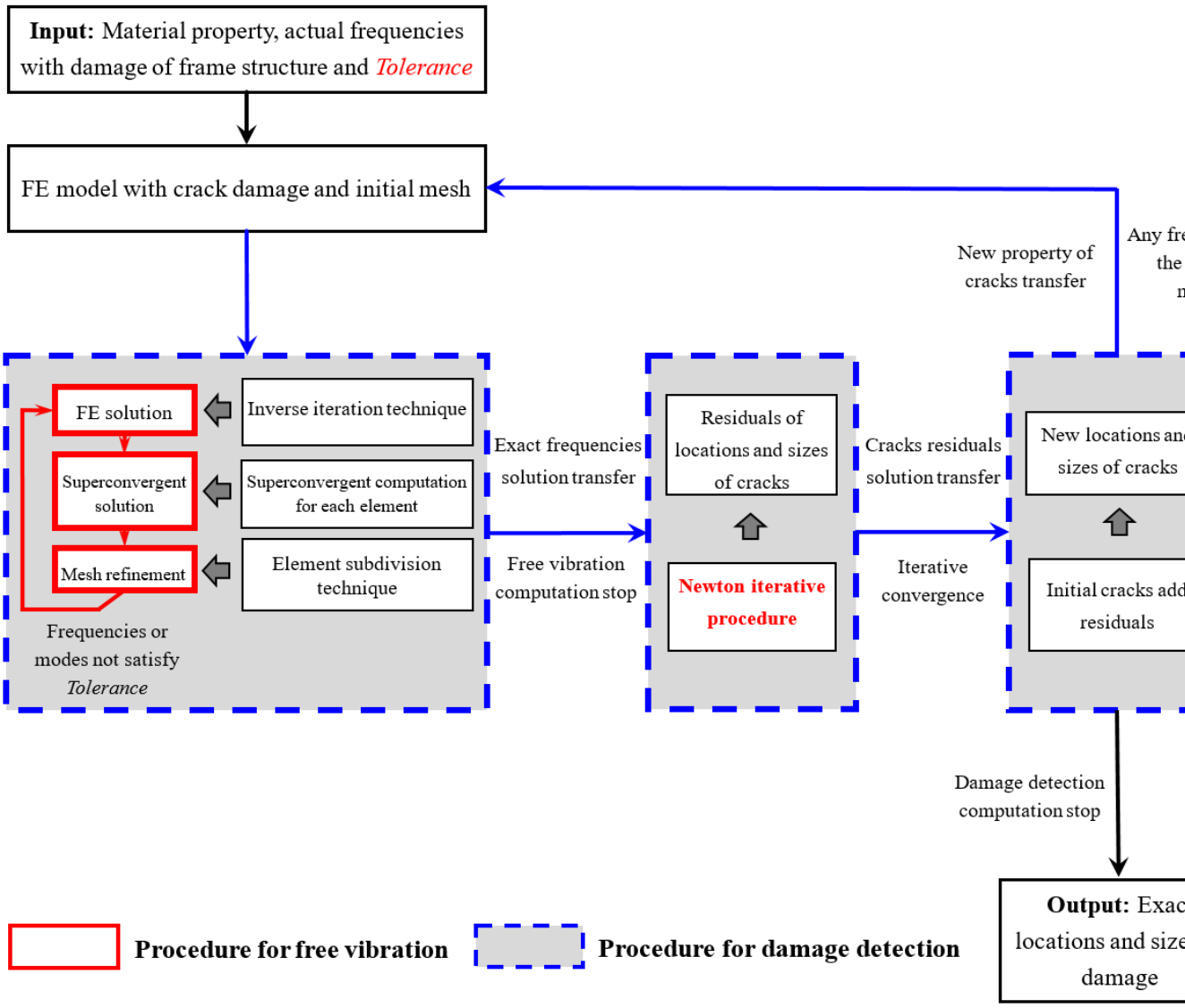

Figure 5. Adaptive FEM algorithm flowchart for free vibration problem (forward eigenproblem) and damage de (inverse eigenproblem).

where $\mathbf{D}$ is the mode vector, and the matrices $\mathbf{K}$ and $\mathbf{M}$ are both independent of ω. The element model adopted is the conventional polynomial element of degree $m > 3$, and $w^h \in C^1$ denotes the conventional FE solution on the given mesh π, in which C^1 is the space of functions that are continuous up to their first-order derivative. As in common practice, the shape functions for w^h are Hermite polynomials. Given an arbitrary trial value ω_a as the shift value, Eq. (6) can be equivalently written in the shifted form (Zienkiewicz and Taylor, 2000)

$$\mathbf{K}_a \mathbf{D} = \mu \mathbf{M} \mathbf{D} \quad \text{with } \mathbf{K}_a = \mathbf{K} - \omega_a^2 \mathbf{M},\ \mu = \omega^2 - \omega_a^2 \tag{7}$$

In the proposed method, the convectional FE computation for eigenpair solutions is based on the Sturm sequence property (Clough and Penzien, 1993), which can be expressed as

$$\mathbf{K} - \omega^2 \mathbf{M} = \mathbf{L}\mathbf{D}(\omega)\mathbf{L}^T \tag{8}$$

where $\mathbf{L}$ is a lower triangular matrix with leading diagonal elements being one, $\mathbf{L}^T$ is its transpose, and $\mathbf{D}(\omega)$ is a diagonal matrix in which the number of eigenvalues less than the arbitrary trial value ω_a equals the number of negative leading diagonal elements in $\mathbf{D}(\omega_a)$. The Rayleigh quotient is used to accelerate the convergence on the eigenvalues:

$$\omega^2 = \frac{\mathbf{D}^T \mathbf{K}\, \mathbf{D}}{\mathbf{D}^T \mathbf{M}\, \mathbf{D}} \tag{9}$$

Utilizing the above Sturm sequence property and the convectional bisection method (Clough and Penzien, 1993), the intervals of each eigenvalue can be determined, and the inverse iteration technique is successfully introduced to compute the eigenpairs (Yuan *et al*., 2013; Yuan *et al*., 2017). Based on these considerations, the following inverse iteration procedure is adopted:

$$\begin{cases} \overline{\mathbf{D}}_{i+1} = \mathbf{K}_a^{-1} \mathbf{M}\, \mathbf{D}_i \\ \mu_{i+1} = \dfrac{\overline{\mathbf{D}}_{i+1}^T \mathbf{M}\, \mathbf{D}_i}{\overline{\mathbf{D}}_{i+1}^T \mathbf{M}\, \overline{\mathbf{D}}_{i+1}} \\ \mathbf{D}_{i+1} = \mathrm{sgn}(\mu_{i+1}) \dfrac{\overline{\mathbf{D}}_{i+1}}{\max(\overline{\mathbf{D}}_{i+1})} \end{cases} \tag{10}$$

where i is the loop index. The above inverse iteration procedure is terminated when the following conditions are met

$$\left| \mu_{i+1} - \mu_i \right| < Tol \quad \text{and} \quad \max \left| \mathbf{D}_{i+1} \right| < Tol \tag{11}$$

After the above inverse iteration converges, an FE solution (μ^h, $\mathbf{D}^h$) (i.e. (ω^h, $\mathbf{D}^h$) where $(\omega^h)^2 = \omega_a^2 + \mu^h$) is obtained. However, the current mesh may not be sufficiently fine, in which case the accuracy of this FE solution must be estimated by a more accurate solution, namely, the superconvergent solution, which is discussed in the following section.

3.2 Error estimation and mesh refinement

The superconvergent patch recovery displacement technique was developed for computation of superconvergent displacements for FE solutions of static and dynamic problems (Wiberg *et al*., 1999a, 1999b). The displacements provided by the superconvergent computation technique can be applied to eigenfunctions. For example, as shown in Figure 6, element e is the superconvergent computation element, and elements e–1 and e+1 are neighbouring elements, in which FE nodes j–1, j, j+1, and j+2 are selected for computation.

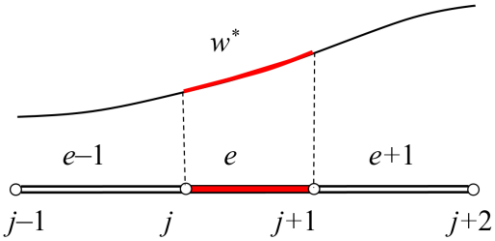

Figure 6. Computation of superconvergent displacements for element e.

The superconvergent displacements for element e can be computed as

$$w^*(x) = \sum_{i=1}^{r} N_i(x) w_i^h + \sum_{i=1}^{s} N_i(x) \overline{w}_i^* \tag{12}$$

where r(=2) is the number of end nodes, s is the number of internal nodes, and $N_i(x)$ is the shape function. The degree of the shape function is improved by one order as $r+s = m+1$. To make the best use of the superconvergent order $O(h^{2m})$ for displacements at end nodes, the displacement recovery field can be expressed by FE nodes as

$$\overline{w}^*(x) = \mathbf{Pa} \tag{13}$$

where $\mathbf{P}$ is the given function vector, and $\mathbf{a}$ can be obtained by the least squares fitting technique for the coincidence of displacements at the end nodes in the recovery field and the conventional FE field. The superconvergent displacements at the end nodes in recovery field $\overline{w}^*(x)$ are used in Eq. (12) to obtain the superconvergent solutions on element e. Because the accuracy of the superconvergent solution w^* is at least one order higher than that of w^h, for elements of degree

$m > 3$, a very simple strategy for error estimation is to use w^* instead of the exact solution w to estimate the errors in w^h. This error estimation method has shown good reliability and effectiveness (Wiberg *et al*., 1999a, 1999b).

The superconvergent solutions of Eq. (13) can be used in the Rayleigh quotient (Clough and Penzien, 1993) to obtain estimates of the eigenvalue:

$$\omega_k^* = \sqrt{\frac{a(w_k^*, w_k^*)}{b(w_k^*, w_k^*)}}, \quad k = 1,2,\mathrm{K}\ ,2n \tag{14}$$

where $a(w,v) = \int_0^l EI(x) w'' v'' \,\mathrm{d}x$ and $b(w,v) = \int_0^l m(x) w v \,\mathrm{d}x$ are the strain energy inner product and the kinematic energy inner product, respectively. The estimated eigenvalue is a stationary value when taken over all possible functions that satisfy the essential BCs. The stationary values computed by Eq. (14) are superconvergent eigenvalues and the corresponding functions ω_k^* are the superconvergent solutions. The Rayleigh quotient, Eq. (14), can be expressed based on elements as

$$\omega_k^* = \sqrt{\frac{\sum_e \int_{a_e}^{b_e} EI(x) w_k^{*\prime\prime} w_k^{*\prime\prime} \,\mathrm{d}x}{\sum_e \int_{a_e}^{b_e} m(x) w_k w_k \,\mathrm{d}x}}, \quad k = 1,2,\mathrm{K}\ ,2n \tag{15}$$

where a_e and b_e are the end nodes of the boundary for element *e*.

Here, each element on the current mesh is divided into a grid of M equal subintervals. For the $M-1$ interior grid points on a typical element *e*, the conventional FE solutions w_g^h and the superconvergent solutions w_g^* at the *g*-th interior point ($g = 1, 2, \Lambda\ , M-1$) are calculated. Then, the errors at the $M-1$ interior points are calculated and estimated to determine if all of them satisfy the given tolerance:

$$\left\| e_{w,k}^* \right\|_e \le Tol \cdot \left[\left(\left\| w_k^h \right\|^2 + \left\| e_{w,k}^* \right\|^2 \right) \Big/ n_e \right]^{1/2}, \quad k = 1,2,\mathrm{K}\ ,2n \tag{16}$$

where $e_{w,k}^*$ is the error of the superconvergent displacements w_k^* and the computed displacements w_k^h, n_e is the number of elements, $\|w\| = [a(w,w)]^{1/2}$. Eq. (16) can be equivalently written in the following form

$$\xi_k = \frac{\left\| e^*_{w,k} \right\|_e}{\bar{e}_{w,k}} \quad \text{with} \quad \bar{e}_{w,k} = Tol \cdot \left[\left(\left\| w^h_k \right\|^2 + \left\| e^*_{w,k} \right\|^2 \right) \Big/ n_e \right]^{1/2}, \quad k = 1,2,\mathrm{K}\ ,2n \tag{17}$$

where ξ_k should satisfy

$$\xi_k \le 1, \quad k = 1,2,\mathrm{K}\ ,2n \tag{18}$$

Usually it is more than sufficient to set M in the range of $4 \le M \le 8$. Therefore, without loss of generality, M is set to 6 for the remainder of this paper.

If Eq. (18) is not satisfied for any interior point, the corresponding element needs to be subdivided into uniform sub-elements by inserting some interior nodes through *h*-refinement (Zienkiewicz and Zhu, 1992a, 1992b; Zienkiewicz *et al*., 2000), which are calculated by

$$h_{k,\mathrm{new}} = \xi_k^{-1/m} h_{k,\mathrm{old}}, \quad k = 1,2,\mathrm{K}\ ,2n \tag{19}$$

where $h_{k,\mathrm{new}}$ is the length of the sub-element, $h_{k,\mathrm{old}}$ is the original length of element *e*, and $\lfloor \cdot \rfloor$ represents the 'floor' operator, i.e. rounding down to the nearest integer. The above element subdivision approach is implemented as

$$n_{k,\mathrm{new}} = \min\left(\left\lfloor \xi_k^{-1/m} \right\rfloor, d \right), \quad k = 1,2,\mathrm{K}\ ,2n \tag{20}$$

where $n_{k,\mathrm{new}}$ is the number of subelements after element subdivision, and d is the limit number for avoiding too many redundant elements. Each element *e* that does not satisfy the pre-specified error tolerance is uniformly subdivided, e.g. $h_{k,\mathrm{new}} = h_{k,\mathrm{old}} / 6$ as shown in Figure 7.

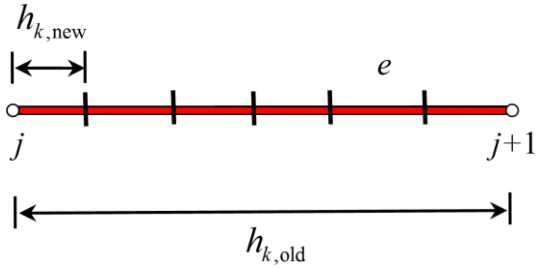

Figure 7. Uniform subdivision of element *e* (e.g. $h_{k,\mathrm{new}} = h_{k,\mathrm{old}} / 6$).

4. NEWTON–RAPHSON ITERATION

Based on the frequency measurement method, the residuals of the frequencies and cracks are consistent with each other; therefore, the Newton–Raphson iteration technique can be introduced (Clough and Penzien, 1993). For the identification of *n* cracks in a beam, there should be 2*n*

unknown crack parameters: α_1, β_1, α_2, β_2,…, α_n, and β_n. To match the number of equations and the number of unknown parameters, it is assumed that 2*n* natural frequency measurements ω_1^0, ω_2^0,…, ω_{2n-1}^0 and ω_{2n}^0 are available in advance. The Newton–Raphson iteration procedure is applied in this paper as follows:

(a) The user assumes initial values of α_1, β_1, α_2, β_2,…, α_n, and β_n and the FE mesh of the beam.

(b) Locate the positions that represent the cracks according to the new crack locations parameters β_1, β_2,…, β_n.

(c) Solve the forward eigenproblem to obtain FE solutions for ω_1^h, ω_2^h,…, ω_{2n}^h with the crack parameters α_1, β_1, α_2, β_2,…, α_n, and β_n, and evaluate the Jacobian matrix

$$\mathbf{J} = \begin{bmatrix} \frac{\partial \omega_1^h}{\partial \alpha_1} & \frac{\partial \omega_1^h}{\partial \beta_1} & \frac{\partial \omega_1^h}{\partial \alpha_2} & \frac{\partial \omega_1^h}{\partial \beta_2} & \Lambda & \frac{\partial \omega_1^h}{\partial \alpha_n} & \frac{\partial \omega_1^h}{\partial \beta_n} \\ \frac{\partial \omega_2^h}{\partial \alpha_1} & \frac{\partial \omega_2^h}{\partial \beta_1} & \frac{\partial \omega_2^h}{\partial \alpha_2} & \frac{\partial \omega_2^h}{\partial \beta_2} & \Lambda & \frac{\partial \omega_2^h}{\partial \alpha_n} & \frac{\partial \omega_2^h}{\partial \beta_n} \\ \mathrm{M} & \mathrm{M} & \mathrm{M} & \mathrm{M} & & \mathrm{M} & \mathrm{M} \\ \frac{\partial \omega_{2n}^h}{\partial \alpha_1} & \frac{\partial \omega_{2n}^h}{\partial \beta_1} & \frac{\partial \omega_{2n}^h}{\partial \alpha_2} & \frac{\partial \omega_{2n}^h}{\partial \beta_2} & \Lambda & \frac{\partial \omega_{2n}^h}{\partial \alpha_n} & \frac{\partial \omega_{2n}^h}{\partial \beta_n} \end{bmatrix} \tag{21}$$

and compute the residuals of frequencies

$$R_k = \omega_k^h - \omega_k^0, \quad k = 1,2,\mathrm{K},2n \tag{22}$$

(d) Solve the following equation by Newton–Raphson iteration:

$$\mathbf{J}\,\mathrm{d}\mathbf{C}^T = -\mathbf{R}^T \tag{23}$$

where $\mathbf{C}^T = (\alpha_1, \beta_1, \alpha_2, \beta_2, \mathrm{K}, \alpha_n, \beta_n)^T$ and $\mathbf{R}^T = (R_1, R_2, \mathrm{K}, R_n)^T$, through which the residuals of n cracks $(\mathrm{d}\alpha_i, \mathrm{d}\beta_i)$ $(i = 1,2,\mathrm{K},n)$ will be obtained.

(e) Update the crack parameters by utilizing the residuals of cracks:

$$(\alpha_i)_{\mathrm{new}} = (\alpha_i)_{\mathrm{old}} + \mathrm{d}\alpha_i, \quad (\beta_i)_{\mathrm{new}} = (\beta_i)_{\mathrm{old}} + \mathrm{d}\beta_i, \qquad i = 1,2,\mathrm{K},n \tag{24}$$

where $(\,)_{\mathrm{new}}$ and $(\,)_{\mathrm{old}}$ represent the new and old cracks in the last step, respectively. Update each old crack with the new one, as shown in Figure 8.

(f) In the new crack condition, return to step (a) and repeat the loop until the residuals of frequencies become sufficiently small.

Note that the FE mesh of conventional FEM for the Newton–Raphson iteration procedure is determinate without mesh refinement. However, the adaptive FE analysis proposed in this paper will have more accurate results and a better convergence rate compared to the conventional FE analysis, which is shown in the numerical examples in Section 7.

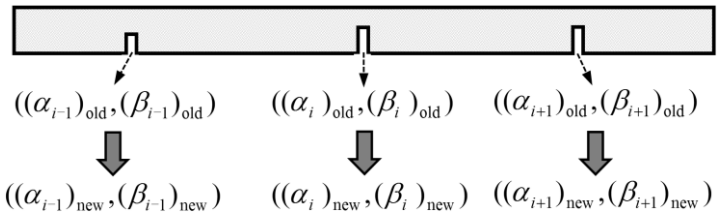

Figure 8. Update of size and location of cracks in one iteration step.

5. DAMAGE REFINEMENT

The matrix elements in the Jacobian matrix **J** are related to the frequencies and crack parameters because the most widely used method, damage detection based on the optimization theory, is reduced to a linearized system of equations. The matrix elements of the Jacobian matrix **J** are the sensitivities of the natural frequencies with respect to the crack parameters. Morassi (2001) developed an explicit expression of the frequency sensitivity to damage, assuming that the sizes of the cracks were sufficiently small. In this study, however, the cracks are not assumed to be small, and the elements of the Jacobian matrix **J** are computed numerically introducing the method by Lee (2009). For example, $\partial\omega_1/\partial\alpha_1$ and $\partial\omega_1/\partial\beta_1$ are computed, respectively, as follows:

$$\frac{\partial\omega_1}{\partial\alpha_1}=\frac{\omega_1(\alpha_1+\delta,\beta_1,\alpha_2,\mathrm{K},\beta_n)-\omega_1(\alpha_1,\beta_1,\alpha_2,\mathrm{K},\beta_n)}{\delta},\qquad |\delta|<<1 \tag{25a}$$

$$\frac{\partial\omega_1}{\partial\beta_1}=\frac{\omega_1(\alpha_1,\beta_1+\delta,\alpha_2,\mathrm{K},\beta_n)-\omega_1(\alpha_1,\beta_1,\alpha_2,\mathrm{K},\beta_n)}{\delta},\qquad |\delta|<<1 \tag{25b}$$

where δ is a value far less than one. Because the crack condition is inaccurate in the initial stage of Newton–Raphson iteration, the residuals of cracks can be adjusted to accelerate the procedure (Lee, 2009). The forward eigenproblem is solved $2n$+1 times per iteration to build the Jacobian matrix **J** and the residuals. To suppress overshoots in the early stage, relaxation is performed during the beginning iterations steps as follows:

$$(\alpha_i)_{\text{new}}=(\alpha_i)_{\text{old}}+0.25\mathrm{d}\alpha_i,\qquad i=1,2,\mathrm{K},n \tag{26a}$$

$$(\beta_i)_{\text{new}}=(\beta_i)_{\text{old}}+0.25\mathrm{d}\beta_i,\qquad i=1,2,\mathrm{K},n \tag{26b}$$

6. ALGORITHMS

The basic algorithm of the proposed adaptive FEM for free vibration problems (forward eigenproblems) is given as follows:

(1) For the k^{th}-order eigenpair (frequency and mode), the initial FE mesh is imported from the final mesh for the previous eigenpair solution, π_{k-1} $(k = 1,2,\text{K},2n)$ (the initial mesh π_0 for the first-order eigenpair and the pre-specified error tolerance Tol are given by user).

(2) For the current order and adaptive step, the FE mesh π_k^t is obtained.

(3) The material properties (i.e. flexural rigidity and linear density) are reduced at the cracks using Eq. (3) to form the whole beam model.

(4) The conventional FE solutions for the eigenpair (ω_k^h, w_k^h) $(k = 1,2,\text{K},2n)$ are computed on the current mesh π_k^t utilizing the inverse iteration procedure of Eq. (10).

(5) Superconvergent FE solutions for eigenpair (ω_k^*, w_k^*) $(k = 1,2,\text{K},2n)$ are computed using the superconvergent patch recovery displacement methodology and Rayleigh quotient of Eqs. (12) and (14), respectively.

(6) The errors of the FE solutions are estimated utilising the superconvergent solutions, in the implementation of the procedure, these errors are estimated at interior points using Eq. (18); if the errors are not satisfied, element subdivision Eq. (20) is used to form the new FE mesh π_k^{t+1}.

(7) The mesh index is updated as $t = t + 1$ and the algorithm returns to step (2) unless the errors are satisfied.

(8) The k^{th}-order mesh is finalized as $\pi_k = \pi_k^t$, the eigenpair index is updated $k = k + 1$, and the algorithm returns to step (1) unless the final order ($k = 2n$) has finished.

Based on the computation of free vibration problems (forward eigenproblems), the global algorithm of the proposed adaptive FEM for damage detection problems (inverse eigenproblems) is proposed as follows:

(1) The actual frequencies of the beam with cracks and initial predicted cracks c_0 are provided, noting that the detection for n cracks needs $2n$ actual frequencies. The initial FE mesh π_0 and the pre-specified error tolerance Tol are given by the user.

(2) Introducing the above basic algorithm for free vibration problems, the conventional FE

solutions for eigenpair (ω_k^h, w_k^h) $(k=1,2,\mathrm{K},2n)$ and superconvergent FE solutions for eigenpair (ω_k^*, w_k^*) $(k=1,2,\mathrm{K},2n)$ on the current mesh are computed. Then the errors of the FE solutions are estimated and the element subdivisions are evolved until the errors are satisfied based on the mesh refinement. Finally, accurate and reliable frequencies of the current crack condition are obtained.

(3) The actual and computed frequencies are compared to analyse their residuals using Eq. (22).

(4) With the Newton–Raphson iteration technique and frequency residuals, the crack residuals are computed using Eq. (23).

(5) With the current crack condition and crack residuals, the new crack condition is computed using Eq. (24).

(6) In the new crack condition, return to step (1) and repeat the loop until the stop criterion in Eq. (5) is satisfied.

7. NUMERICAL EXAMPLES

The proposed adaptive strategy has been coded into a Fortran 90 program; in this section, it was verified by solving four representative numerical examples for free vibration problems, on the other hand, which examples are also selected as damage detection problems to show that the method is correct and competitive. Also, for comparison, whenever needed, both the free vibration and damage detection problems are dealt with together by setting one-to-one corresponding examples respectively, e.g. Example 1 and Example 5 cases. All of these examples were run utilizing the Intel(R) Visual Fortran Compiler on a DELL Optiplex 380 desktop computer with an Intel(R) Core(TM) 2.93 GHz CPU, with double-precision floating-point numbers (approximately 14 decimal digits). For all the examples, the tolerance Tol is set to 10^{-3} and the fifth-order ($m=5$) polynomials are used for each element.

For free vibration problems, the error of the computed frequency ω^h is

$$\varepsilon_\omega = \frac{\left|\omega - \omega^h\right|}{1+\left|\omega\right|} \tag{27}$$

where ω is the exact frequency or a reliable result obtained through other methods. The first example is a double-clamped non-uniform uncracked beam, whose exact solution can be computed using SLUTH (Greenberg and Marletta, 1997) with a strict tolerance setting of 10^{-9}.

Therefore, the results obtained from the present method are compared with these exact solutions. For the other three examples, only the calculated results from other studies are available because exact solutions are not available for cracked beams. Every eigenfunction solution shown below is normalized to its biggest value.

For damage detection, the errors of the computed crack depth α^h and location β^h are

$$\varepsilon_\alpha = \frac{|\alpha - \alpha^h|}{1+|\alpha|}, \qquad \varepsilon_\beta = \frac{|\beta - \beta^h|}{1+|\beta|} \tag{28}$$

where α and β are the exact crack depth and location or reliable results obtained through other methods. For all the examples, it was found that the present procedure produced satisfactory results, with both locations and sizes of cracks fully satisfying the pre-specified error tolerance.

7.1 Free vibration problems

Example 1: *Double–clamped uncracked beam with a sinusoidal cross section*

Figure 9(a) shows the double-clamped uncracked beam, and the material data are

$$h(x) = h_0(1 + 0.5\sin(10\frac{x}{l})), \quad m(x) = \rho b h(x), \quad EI(x) = \frac{Ebh^3(x)}{12} \tag{29}$$

This example was selected to check the reliability of the proposed method for non-uniform uncracked beams. The first ten frequencies and the final adaptive mesh computed by the proposed method are shown in Table II. This table also displays the solutions computed using SLEUTH with a strict tolerance setting of 10^{-9}, which serves as the exact solution because this problem does not have an analytic solution. It is evident that the pre-specified error tolerance is well satisfied for frequencies. The first three computed modes are shown in Figure 9(b); clearly, the vibration becomes more complicated as the order increases, which means that more elements are necessary to effectively analyse the free vibration problem, as shown in Table II.

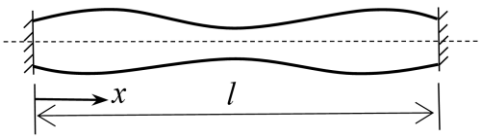

(a)

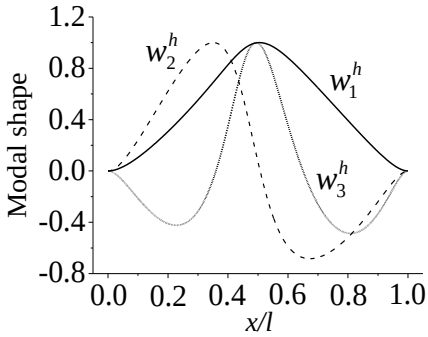

(b)

Figure 9. Model and modes of Example 1. **Notes:** (a) Double-clamped uncracked beam with a sinusoidal cross section. (b) Computed results for first three modes.

Table II. Computed results for frequencies of Example 1.

	Present method			SLEUTH solutions
k	ω_k^h	ε_ω	Elements	ω_k
1	21.446122	7.97E-04	7	21.428254
2	56.805177	2.84E-05	9	56.803537
3	124.219103	6.28E-05	9	124.211235
4	196.270778	5.59E-04	9	196.160646
5	293.647288	2.49E-05	12	293.639963
6	411.989517	1.30E-05	12	411.984134
7	550.268718	2.21E-05	12	550.256549
8	708.331094	9.42E-06	16	708.324415
9	886.135673	5.20E-06	16	886.131057
10	1083.668240	4.66E-06	20	1083.663183

Example 2: *Stepped cantilever beam with a single crack*

Figure 10(a) shows the stepped cantilever beam with a single crack with lengths l_1 and l_2, heights h_1 and h_2, and the following material data

$$l_1 = l_2 = 0.25\text{m}, \quad E = 2.1\times10^{11}\,\text{Pa}, \quad \rho = 7800\,\text{kg/m}^3, \quad \nu = 0.3. \tag{30}$$

This model was previously analysed using a semi-analytical method (Nandwana and Maiti, 1997). Three cases are considered, as shown in Table III, for different sizes of cracks and different beam heights. The first four computed frequencies are shown in Table III. Therein, the results of the present method are compared with the solutions with the semi-analytical method for $h_1 = 0.02\text{m}$ and $h_2 = 0.16\text{m}$ as Cases (a) and (b). Furthermore, the frequencies were computed for a large step ratio $h_1 = 0.02\text{m}$ and $h_2 = 0.16\text{m}$ in Case (c) to check the stability of the proposed method; the exact solution for Case (c) was calculated using the proposed method with a strict tolerance setting of 10^{-9}. The computed solutions are consistent with the semi-analytical solutions for Cases (a) and (b); furthermore, the computed solutions for Case (c) using the pre-specified error tolerance $Tol = 10^{-3}$ agree with the solutions using the strict tolerance of 10^{-9}. The first three computed modes of Case (c) are shown in Figure 10(b). This figure shows that the modes

become more complicated in the domain of relatively small stiffness. For further consideration, the 10th-order modes for Cases (a) and (c) are shown in Figs. 11(a) and (b), respectively. In these figures, the final adaptive mesh is shown as tick marks on the horizontal axis. Because the stiffness is fairly constant in Case (a), the modes are smooth and the mesh is fairly uniform. In contrast, because the left half of the beam in Case (c) is much stiffer, the mode varies significantly throughout the beam, and a finer mesh is required near the tip of the beam.

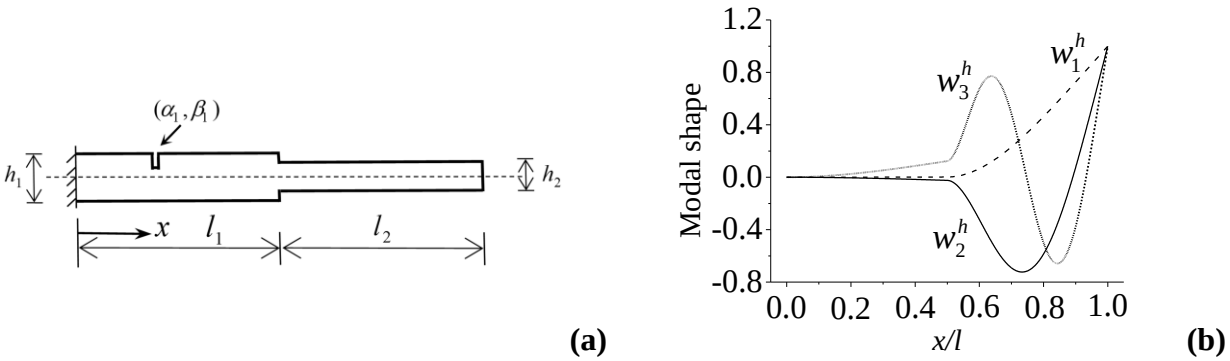

Figure 10. Model and modes of Example 2. **Notes:** (a) Stepped cantilever beam with single crack. (b) Computed results for first three modes of Case(c).

Table III. Computed results for frequencies of Example 2. **Source:** [a] Results from paper Nandwana and Maiti (1997)

Cracks		k	Present method		Results [a] (Cases (a) & (b))
			ω_k^h	ε_ω	ω_k
Case (a)	$\alpha_1 = 0.100$ $\beta_1 = 0.200$ $h_1 = 0.02\text{m}$ $h_2 = 0.016\text{m}$	1	457.308321	9.49E-03	453.0
		2	2376.679751	1.32E-02	2345.7
		3	6649.213179	2.32E-02	6498.4
		4	12790.812926	——	——
Case (b)	$\alpha_1 = 0.200$ $\beta_1 = 0.200$ $h_1 = 0.02\text{m}$ $h_2 = 0.016\text{m}$	1	457.308321	4.24E-02	477.6
		2	2376.679751	1.37E-02	2344.6
		3	6649.213179	2.60E-02	6480.9
		4	12790.812926	——	——
Case (c)	$\alpha_1 = 0.100$ $\beta_1 = 0.200$ $h_1 = 0.20\text{m}$ $h_2 = 0.016\text{m}$	1	1344.066976	4.97E-04	1344.736216
		2	8300.314483	1.44E-04	8301.508858
		3	16333.267628	6.07E-04	16323.357462
		4	24216.911236	1.31E-04	24220.074496

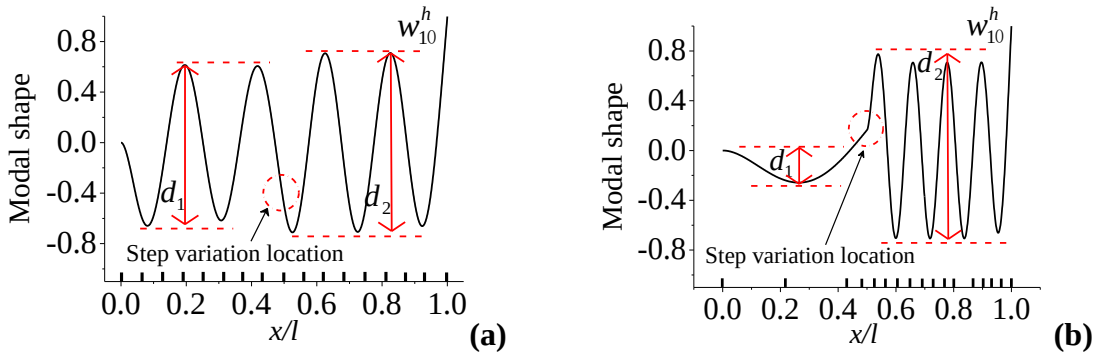

Figure 11. Computed 10th-order modes for different stepped height ratios and final meshes in Example 2. **Notes:** (a) Case (a). (b) Case (c).

Example 3: *Cantilever beam with double cracks*

Figure 12(a) shows a cantilever beam with two cracks, and the material data are

$$l = 0.5\,\text{m}, \quad h = 0.02\,\text{m}, \quad E = 2.1\times10^{11}\,\text{Pa}, \quad \rho = 7860\,\text{kg/m}^3, \quad \nu = 0.3. \tag{31}$$

This example was selected to check the reliability of the proposed method for computing the frequencies and corresponding modes of beams with multiple cracks. This model was previously analysed using the torsional spring method for simulating the cracks (Lee, 2009). Three cases were considered, as shown in Table IV for different locations and sizes of cracks. The first four computed frequencies are shown in Table IV. These solutions are compared with the solutions from the torsional spring method. The computed solutions are consistent with the torsional spring method for the three cases. The first three computed modes for Case (c) are shown in Figure 12(b).

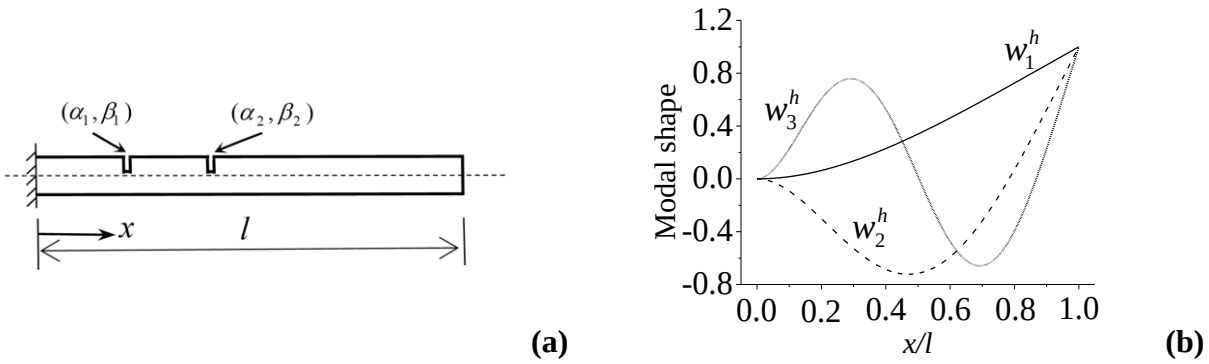

Figure 12. Model and modes of Example 3. **Notes:** (a) Cantilever beam with two cracks. (b) Computed results for the first three modes of Case (c).

Table IV. Computed results for frequencies of Example 3. **Source:** [a] Results from paper Lee (2009)

Cracks		k	Present method		Results [a]
			ω_k^h	ε_ω	ω_k
Case (a)	$\alpha_1 = 0.1$	1	419.709187	6.29E-03	417.0794
	$\beta_1 = 0.2$	2	2630.272577	3.01E-03	2622.389
	$\alpha_2 = 0.1$	3	7364.839379	3.20E-03	7341.322
	$\beta_2 = 0.4$	4	14432.145781	4.45E-03	14368.22
Case (b)	$\alpha_1 = 0.1$	1	419.709187	3.56E-03	418.2175
	$\beta_1 = 0.4$	2	2630.272577	1.82E-02	2583.284
	$\alpha_2 = 0.2$	3	7364.839379	1.09E-02	7285.600
	$\beta_2 = 0.6$	4	14432.145781	4.02E-03	14374.36
Case (c)	$\alpha_1 = 0.1$	1	419.709187	5.86E-04	419.4628
	$\beta_1 = 0.6$	2	2630.272577	6.99E-03	2612.009
	$\alpha_2 = 0.2$	3	7364.839379	1.43E-02	7260.865
	$\beta_2 = 0.8$	4	14432.145781	1.94E-02	14158.15

Example 4: *Cantilever beam with triple cracks*

Figure 13(a) shows a cantilever beam with three cracks; the material data are the same as Example 3. Three cases were considered as shown in Table V for different locations and sizes of cracks. The first six computed frequencies are shown in Table V. These solutions are compared with the solutions from the torsional spring method for Cases (a) and (b). Similar to Example 2, exact solutions were obtained for Case (c) using the proposed method with a strict tolerance of 10^{-9}. In Case (c), the frequencies were computed for deep cracks to check the stability of the proposed method. The computed solutions are consistent with the torsional spring method for Cases (a) and (b), and the solutions computed with the pre-specified error tolerance $Tol = 10^{-3}$ match the solutions with the tolerance of 10^{-9}. The first three computed modes of the deep cracks for Case (c) are shown in Figure 13(b). This figure shows that the modes become more complicated as the cracks deepen. For further consideration, uncracked and deeply cracked beams are compared in Figs. 14(a) and (b), respectively. In these figures, the final adaptive mesh is shown as tick marks on the horizontal axis. Because there are no cracks in the case shown in Figure 14(a), the modes are smooth and the mesh is fairly uniform. In contrast, the cracks in the case shown in Figure 14(b)

cause the mode to grow in magnitude as it passes through the cracks, and a finer mesh is necessary in the vicinity of the cracks.

Table V. Computed results for frequencies of Example 4. **Source:** [a] Results from paper Lee (2009)

Cracks		k	Present method		Results [a]
			ω_k^h	ε_ω	ω_k
Case (a)	$\alpha_1 = 0.1$	1	419.709187	6.74E-03	416.8933
	$\beta_1 = 0.2$	2	2630.272577	6.97E-03	2612.065
	$\alpha_2 = 0.1$	3	7364.839379	5.59E-03	7323.879
	$\beta_2 = 0.4$	4	14423.380407	4.65E-03	14356.68
	$\alpha_3 = 0.1$	5	23823.591113	9.91E-03	23589.91
	$\beta_3 = 0.6$	6	35634.541339	8.59E-04	35603.94
Case (b)	$\alpha_1 = 0.1$	1	419.709187	6.32E-03	417.0652
	$\beta_1 = 0.2$	2	2630.272577	3.78E-03	2620.375
	$\alpha_2 = 0.1$	3	7364.839379	6.34E-03	7318.436
	$\beta_2 = 0.4$	4	14415.115577	8.05E-03	14299.97
	$\alpha_3 = 0.1$	5	23824.135951	9.48E-03	23600.29
	$\beta_3 = 0.8$	6	35630.346532	1.59E-03	35573.62
Case (c)	$\alpha_1 = 0.3$	1	419.809187	2.38E-04	417.332753
	$\beta_1 = 0.2$	2	2630.309132	1.39E-05	2616.921931
	$\alpha_2 = 0.3$	3	7364.539463	4.07E-05	7335.876113
	$\beta_2 = 0.4$	4	14432.168001	1.54E-06	14377.867894
	$\alpha_3 = 0.3$	5	23657.374210	4.45E-05	23658.501681
	$\beta_3 = 0.6$	6	35638.841304	7.15E-04	35613.380555

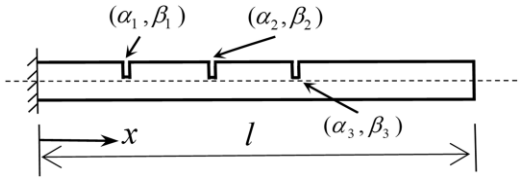

(a)

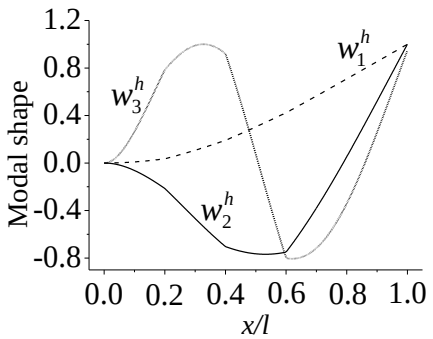

(b)

Figure 13. Model and modes of Example 4. **Notes:** (a) Cantilever beam with three cracks. (b) Computed results for first three modes of Case (c).

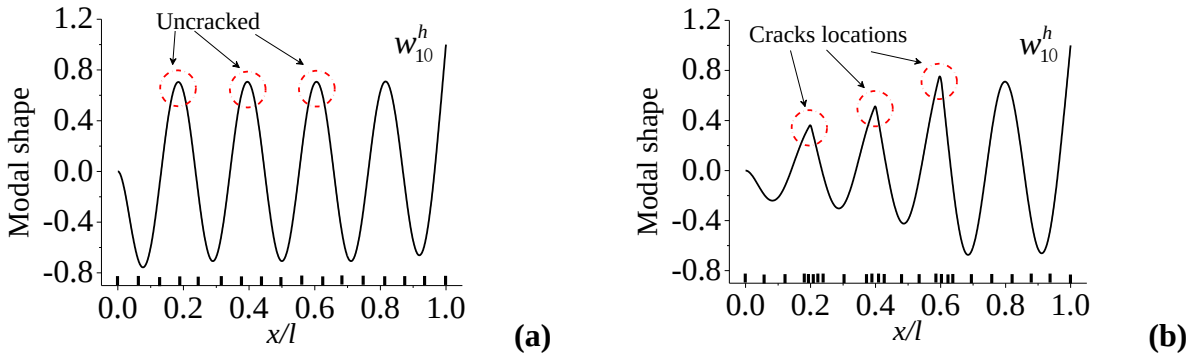

Figure 14. Tenth-order computed modes and final meshes for different crack sizes in Example 4. **Notes:** (a) Uncracked beam: $\alpha_i = 0.0\,(i = 1, 2, 3)$. (b) Deeply cracked beam: $\alpha_i = 0.3\,(i = 1, 2, 3)$.

7.2 Damage detection problems

Example 5: *Double–clamped uncracked beam with a sinusoidal cross section*

Consider the clamped-clamped uncracked beam in Figure 15(a) and the material data are the same as Example 1 as shown in Eq. (29). This example is selected for checking the reliability of the proposed method for non-uniform uncracked beams. Because exact frequencies do not exist in this case, the first four frequencies of forward eigenproblems computed by the proposed method are used as actual frequencies, as listed in Table VI. Assuming the existence of two cracks, the first four frequencies and crack properties computed by the proposed method are listed in Table VI. It can be seen that the two detected cracks are located at $\beta_1 = 0.15224$ and $\beta_2 = 0.65163$, and the differences between the computed and actual sizes (0.000) of the cracks satisfy the pre-specified error tolerance $Tol = 10^{-3}$, revealing that there are no cracks in this non-uniform beam. In Table VI, the differences between the computed and actual frequencies also satisfy the pre-specified error tolerance. The Newton–Raphson iteration results for cracks are shown in Figure 15(b), where the Newton–Raphson iteration converges after only 6 iteration steps.

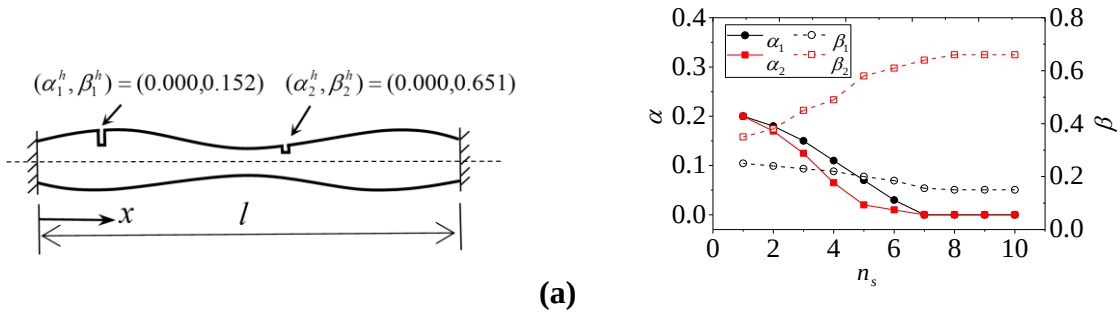

Figure 15. Model and damage detection results of Example 5. **Notes:** (a) Clamped-clamped beam with sinusoidal cross section. (b) Newton–Raphson iteration results for cracks.

Example 6: *Stepped cantilever beam with a single crack*

Consider the stepped cantilever beam with a single crack in Figure 16(a) with lengths l_1 and l_2, heights h_1 and h_2, and the material data are the same as Example 2 as shown in Eq. (30). This model had been analysed by a semi-analytical method (Nandwana and Maiti, 1997). Considering three cases with different locations and sizes of cracks as $\alpha_1 = 0.100$, $\beta_1 = 0.200$ and $\alpha_1 = 0.200$, $\beta_1 = 0.200$, the first four computed frequencies are listed in Table VII and compared with the solutions obtained using the semi-analytical method for $h_1 = 0.02\text{m}$ and $h_2 = 0.16\text{m}$ as case (a) and case (b). On the other hand, the frequencies were computed for a large step ratio with $h_1 = 0.20\text{m}$ and $h_2 = 0.016\text{m}$ as case (c). The first four frequencies of forward eigenproblems computed by the proposed method, considered as the actual frequencies, are listed in Table VII. Assuming the existence of two cracks, the first four frequencies and crack properties computed by the proposed method are also listed in Table VII. It can be seen that the two detected cracks are located at $\alpha_1 = 0.100$, $\beta_1 = 0.200$ and $\alpha_1 = 0.200$, $\beta_1 = 0.200$, and the differences between the computed and actual sizes of the cracks satisfy the pre-specified error tolerance, revealing that there is only one crack in this non-uniform beam. In Table VII, the differences between computed and actual frequencies also satisfy the pre-specified error tolerance. The Newton–Raphson iteration results for cracks are shown in Figure 16(b), where the Newton–Raphson iteration converges after only 6 iteration steps as in Example 5. The final meshes of the 4th order for different Newton–Raphson iteration steps are shown in Figure 17, where the domain near the cracks needs more elements in the 1st, 3rd, and 7th iteration steps.

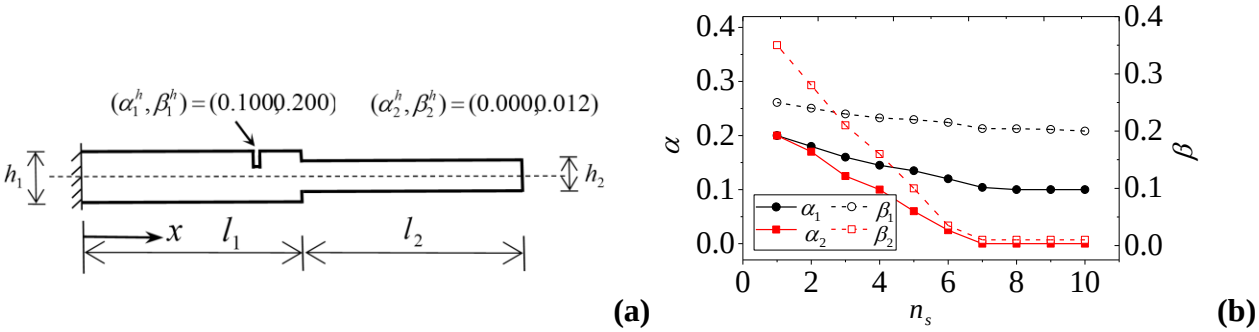

Figure 16. Model and damage detection results for Example 6. **Notes:** (a) Stepped cantilever beam with a single crack. (b) Newton–Raphson iteration results for cracks.

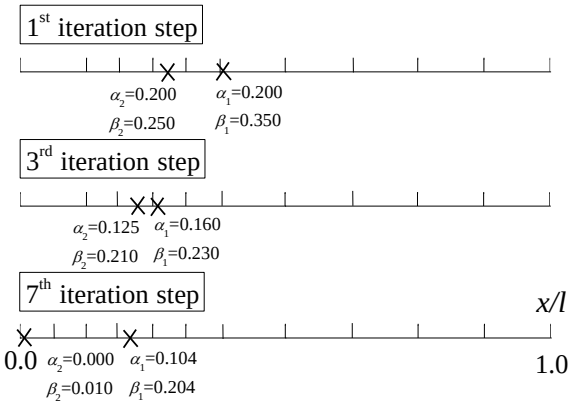

Figure 17 Final meshes of the 4th order computed results for different Newton–Raphson iteration steps of Example 6 (symbol '×' represents the crack).

Example 7: *Cantilever beam with double cracks*

Consider the cantilever beam with two cracks in Fig. 18(a) and the material data are the same as Example 3 as shown in Eq. (31). This model had been analysed by the torsional spring model method for simulating the cracks (Lee, 2009). Considering different locations and sizes of cracks as case (a) $\alpha_1 = 0.1$, $\beta_1 = 0.2$, $\alpha_2 = 0.1$, $\beta_2 = 0.4$; case (b) $\alpha_1 = 0.1$, $\beta_1 = 0.4$, $\alpha_2 = 0.2$, $\beta_2 = 0.6$; and case (c) $\alpha_1 = 0.1$, $\beta_1 = 0.6$, $\alpha_2 = 0.2$, $\beta_2 = 0.8$, the first four computed frequencies are listed in Table VIII and compared with the solutions obtained with the torsional spring model method. The first four frequencies of forward eigenproblems computed by the proposed method, considered as the actual frequencies, are listed in Table VIII. In Table VIII, the differences between the computed and actual frequencies satisfy the pre-specified error tolerance. The Newton–Raphson iteration results of 6 iteration steps for cracks are shown in Figure 18(b), which demonstrates that the proposed method yields a higher convergence rate compared to the conventional FE analysis (Lee, 2009).

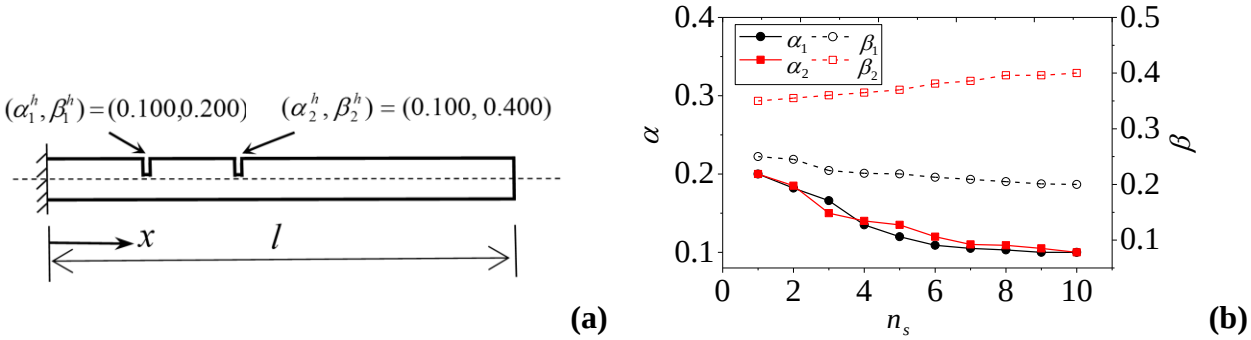

Figure 18. Model and damage detection results for Example 7. **Notes:** (a) Cantilever beam with double cracks. (b) Newton–Raphson iteration results for cracks.

Table VI. Computed results for cracks and frequencies of Example 5.

Cracks	Present method		Actual cracks	k	Present method		
	Computed cracks ε_α and ε_β				ω_k^h	ε_ω	$\omega_k\,(Tol=10^{-3})$
α_1	0.00026	0.26E-3	0.000	1	21.42747	8.31E-04	21.446122
β_1	0.15224	——	——	2	56.80232	4.94E-05	56.805177
α_2	0.00059	0.59E-3	0.000	3	124.21091	6.54E-05	124.219103
β_2	0.65163	——	——	4	196.15611	5.81E-04	196.270778

Table VII. Computed results for cracks and frequencies of Example 6.

Cracks		Present method			k	Present method		
		Computed cracks ε_α and ε_β		Actual cracks		ω_k^h	ε_ω	$\omega_k\,(Tol=10^{-3}$
Case (a)	α_1	0.10061	5.55E-04	0.100	1	457.334903	5.80E-05	457.308321
	β_1	0.20044	3.67E-04	0.200	2	2376.781991	4.30E-05	2376.679751
	α_2	0.00059	5.90E-04	0.000	3	6649.372784	2.40E-05	6649.213179
	β_2	0.01214	——	——	4	12797.592587	5.30E-04	12790.81292
Case (b)	α_1	0.19931	5.75E-04	0.200	1	457.318404	2.20E-05	457.308321
	β_1	0.20023	1.92E-04	0.200	2	2376.708283	1.20E-05	2376.679751
	α_2	0.00015	1.50E-04	0.000	3	6651.540754	3.50E-04	6649.213179
	β_2	0.98124	——	——	4	12791.746728	7.30E-05	12790.81292
Case (c)	α_1	0.10085	7.73E-04	0.100	1	1344.073836	5.10E-06	1344.066976
	β_1	0.20046	3.83E-04	0.200	2	8300.430701	1.40E-05	8300.314483
	α_2	0.00049	4.90E-04	0.000	3	16335.391083	1.30E-04	16333.26762
	β_2	0.35243	——	——	4	24217.783081	3.60E-05	24216.91123

Table VIII. Computed results for cracks and frequencies of Example 7.

Cracks		Present method			k	Present method		
		Computed cracks ε_α and ε_β		Actual cracks		ω_k^h	ε_ω	$\omega_k\,(Tol=10$
Case (a)	α_1	0.10026	2.36E-04	0.100	1	419.839607	3.10E-04	419.70918
	β_1	0.20085	7.08E-04	0.200	2	2630.433085	6.10E-05	2630.27257
	α_2	0.10032	2.91E-04	0.100	3	7365.170842	4.50E-05	7364.83937
	β_2	0.40015	1.07E-04	0.400	4	14437.341713	3.60E-04	14432.1457
Case (b)	α_1	0.10012	1.09E-04	0.100	1	419.759672	1.20E-04	419.70918
	β_1	0.39956	3.14E-04	0.400	2	2630.496235	8.50E-05	2630.27257
	α_2	0.20010	8.33E-05	0.200	3	7365.119281	3.80E-05	7364.83937
	β_2	0.60015	9.37E-05	0.600	4	14432.997337	5.90E-05	14432.1457
Case (c)	α_1	0.10045	4.09E-04	0.100	1	419.710617	3.40E-06	419.70918
	β_1	0.60082	5.13E-04	0.600	2	2630.304152	1.20E-05	2630.27257
	α_2	0.19971	2.42E-04	0.200	3	7365.111915	3.70E-05	7364.83937
	β_2	0.80036	2.00E-04	0.800	4	14444.846949	8.80E-04	14432.1457

Example 8: *Cantilever beam with triple cracks*

Consider the cantilever beam with three cracks in Figure 19(a) with the same material data as Example 7. Three cases are considered for different locations and sizes of cracks as case (a) $\alpha_1 = 0.1$, $\beta_1 = 0.2$, $\alpha_2 = 0.1$, $\beta_2 = 0.4$, $\alpha_3 = 0.1$, $\beta_3 = 0.6$; case (b) $\alpha_1 = 0.1$, $\beta_1 = 0.2$, $\alpha_2 = 0.1$, $\beta_2 = 0.4$, $\alpha_3 = 0.1$, $\beta_3 = 0.8$; and case (c) $\alpha_1 = 0.3$, $\beta_1 = 0.2$, $\alpha_2 = 0.3$, $\beta_2 = 0.4$, $\alpha_3 = 0.3$, $\beta_3 = 0.6$. The first six frequencies of forward eigenproblems computed by the proposed method are listed in Table IX and compared with the solutions obtained using the torsional spring model method. In Table IX, the differences between the computed and actual frequencies satisfy the pre-specified error tolerance. The Newton–Raphson iteration results for cracks are shown in Figure 19(b), where the Newton–Raphson iteration converges after 6 iteration steps as in the above three examples, demonstrating that the proposed method yields a higher convergence rate compared to the conventional FE analysis (Lee, 2009). The final meshes of the 6th order for different Newton–Raphson iteration steps are shown in Figure 20, where the domain near the cracks needs more elements in the 1st, 3rd, and 7th iteration steps. Furthermore, the adaptive FE procedure makes mesh refinement possible.

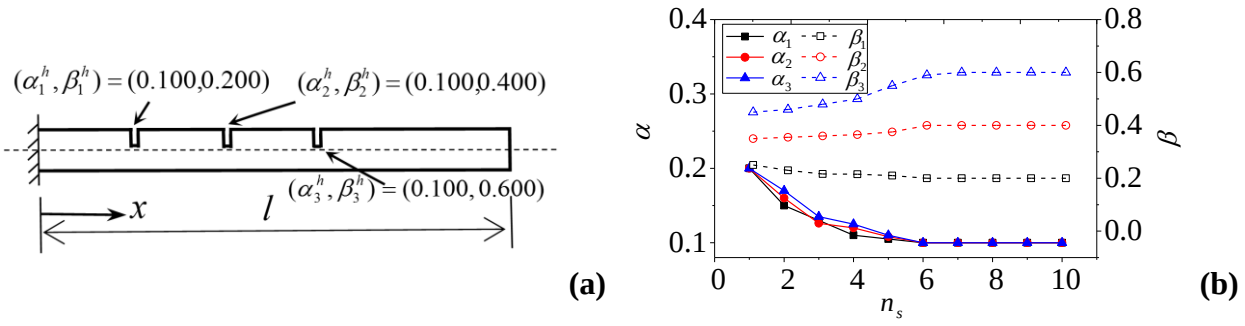

Figure 19. Model and damage detection results for Example 8. **Notes:** (a) Cantilever beam triple cracks. (b) Newton–Raphson iteration results for cracks.

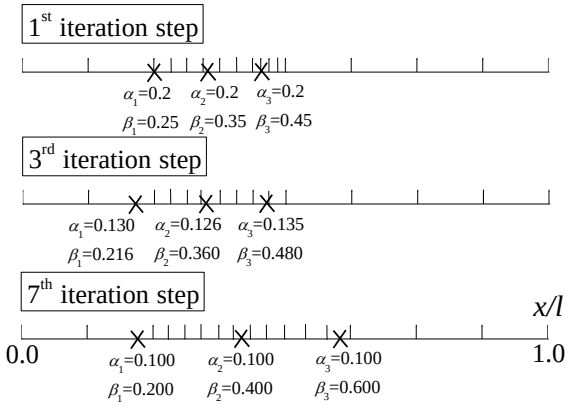

Figure 20. Final meshes of the 6th order computed results for different Newton–Raphson iteration steps of Example 8 (symbol '×' represents the crack).

Table IX. Computed results for cracks and frequencies of Example 8.

Cracks		Present method		Actual cracks	k	Present method		
		Computed cracks ε_α and ε_β				ω_k^h	ε_ω	ω_k (
Case (a)	α_1	0.09952	4.36E-04	0.100	1	419.720125	0.26E-4	41
	β_1	0.20036	3.00E-04	0.200	2	2630.301521	0.11E-4	263
	α_2	0.10051	4.64E-04	0.100	3	7366.312547	0.20E-3	736
	β_2	0.39926	5.29E-04	0.400	4	14423.899685	0.36E-4	144
	α_3	0.10082	7.45E-04	0.100	5	23839.791835	0.68E-3	238
	β_3	0.60012	7.50E-05	0.600	6	35636.144938	0.45E-4	356
Case (b)	α_1	0.10064	5.82E-04	0.100	1	419.715498	0.15E-4	41
	β_1	0.20076	6.33E-04	0.200	2	2630.314677	0.16E-4	263
	α_2	0.09994	5.45E-05	0.100	3	7371.100342	0.85E-3	736
	β_2	0.40026	1.86E-04	0.400	4	14415.432732	0.22E-4	144
	α_3	0.10014	1.27E-04	0.100	5	23832.713000	0.36E-3	238
	β_3	0.79812	1.04E-03	0.800	6	35631.843049	0.42E-4	356
Case (c)	α_1	0.30026	2.00E-04	0.300	1	419.815499	0.15E-4	41
	β_1	0.20014	1.17E-04	0.200	2	2630.506480	0.75E-4	263
	α_2	0.29881	9.15E-04	0.300	3	7369.768996	0.71E-3	736
	β_2	0.40011	7.86E-05	0.400	4	14432.355632	0.13E-4	144
	α_3	0.30023	1.77E-04	0.300	5	23660.686382	0.14E-3	236
	β_3	0.60074	4.63E-04	0.600	6	35641.050974	0.62E-4	356

8. CONCLUSIONS

In this study, a new adaptive FEM methodology was presented for accurate computation of both the frequencies and modes of cracked Euler–Bernoulli beams, and the adaptive analysis technology has been developed and applicated for the reliable computation of the locations and sizes of multiple cracks. Some key techniques are utilized, i.e., adaptive FE analysis for eigensolutions, Newton–Raphson iteration, and damage refinement techniques, based on the conventional frequency measurement method for damage detection, which has yielded a simple and practical adaptive FE procedure that finds sufficiently fine meshes for the accurate locations and sizes of multiple cracks to match the pre-specified error tolerance. Numerical examples are provided, including ones known to be representative of a non-uniform and geometrically stepped Euler–Bernoulli beam with multiple cracks, to demonstrate the accuracy, reliability, and effectiveness of the proposed adaptive FE algorithm and procedure. Based on frequency measurements for damage detection, the inverse eigenproblem computation makes full use of the forward eigenproblem computation for frequency solutions. As a result, making the two forward and inverse complementary parts of the research series work together, the proposed FE procedure reduces the cost of computation and improves the accuracy of the solutions for determining the locations and sizes of cracks in beams. The present paper is limited to Euler–Bernoulli beam beams with cracks, but with conventional numerical treatments of integration of beams, the present method can also solve some frame structure problems in an indirect way. Looking forward, a very welcoming and encouraging feature of this presented methodology is that it can readily be extended to damage detection problems of frame structure with multiple cracks as engineering practice, which will be addressed in future papers.

REFERENCES

1. Wang, Z, Lin, R.M. and Lim, M.K. (1997), "Structural damage detection using measured FRF data", *Computer Methods in Applied Mechanics and Engineering*, Vol. 147, No. 1–2, pp. 187–197.
2. Hassiotis, S. and Jeong, G. D. (1993), "Assessment of structural damage from natural frequency measurements", *Computers and Structures*, Vol. 49, No. 4, pp. 679–691.
3. Pawar, P.M. and Ganguli, R. (2003), "Genetic fuzzy system for damage detection in beams and helicopter rotor blades", *Computer Methods in Applied Mechanics and Engineering*, Vol. 192, No. 16–18, pp. 2031–2057.
4. Zacharias, J and Hartmann, C. and Delgado, A. (2004), "Damage detection on crates of beverages by artificial neural networks trained with finite-element data", *Computer Methods in Applied Mechanics and Engineering*, Vol. 193, No. 6–8, pp. 561–574.
5. Yan, W., Chen, W.Q., Cai, J.B. and Lim, C.W. (2007), "Quantitative structural damage detection using high-frequency piezoelectric signatures via the reverberation matrix method", International *Journal for Numerical Methods in Engineering*, Vol. 71, No. 5, pp. 505–528.
6. Farrar, C.R., Doebling, S.W. and Nix, D.A. (2001), "Vibration-based structural damage identification, *Philosophical Transactions of the Royal Society*, Vol. 359, No. 1778, pp. 131–149.
7. Wang, D., Liu, W. and Zhang, H. (2015), "Superconvergent isogeometric free vibration analysis of Euler–Bernoulli beams and Kirchhoff plates with new higher order mass matrices", *Computer Methods in Applied Mechanics and Engineering*, Vol. 286, pp. 230–267.
8. Kaveh, A. and Dadfar, B. (2007), "Eigensolution for free vibration of planar frames by weighted graph symmetry", *International Journal for Numerical Methods in Engineering*, Vol. 69, No. 6, pp. 1305–1330.
9. Litewka, P. and Rakowski, J. (2001), "Free vibrations of shear-flexible and compressible arches by FEM", *International Journal for Numerical Methods in Engineering*, Vol. 52, No. 3, pp. 273–286.
10. Labib, A., Kennedy, D. and Featherston, C. (2014), "Free vibration analysis of beams and frames with multiple cracks for damage detection", *Journal of Sound and Vibration*, Vol. 333, No. 20, pp. 4991–5003.
11. Nandwana, B.P. and Maiti, S.K. (1997), "Detection of the location and size of a crack in

stepped cantilever beams based on measurements of natural frequencies", *Journal of Sound and Vibration*, Vol. 203, No. 3, pp. 435–446.

12. Chaudhari, T.D. and Maiti, S.K. (2000), "A study of vibration of geometrically segmented beams with and without crack", *International Journal of Solids and Structures*, Vol. 37, No. 5, pp. 761–779.
13. Greenberg, L. and Marletta, M. (1997), "Algorithm 775: The code SLEUTH for solving fourth order Sturm–Liouville problems", *ACM Transactions on Mathematical Software*, Vol. 23, No. 4, pp. 453–493.
14. Caddemi, S. and Morassi, A. (2013), "Multi-cracked Euler–Bernoulli beams: mathematical modeling and exact solutions", *International Journal of Solids and Structures*, Vol. 50, No. 6, pp. 944–956.
15. Caddemi, S. and Caliò, I. (2014), "Exact reconstruction of multiple concentrated damages on beams", *Acta Mechanica*, Vol. 225, No. 11, pp. 3137–3156.
16. Hsu, M.H. (2005), "Vibration analysis of edge-cracked beam on elastic foundation with axial loading using the differential quadrature method", *Computer Methods in Applied Mechanics and Engineering*, Vol. 194, No. 1, pp. 1–17.
17. Rizos, P.F., Aspragathos, N. and Dimarogonas, A.D. (1990), "Identification of crack location and magnitude in a cantilever beam from the vibration modes", *Journal of Sound and Vibration*, Vol. 138, No. 3, pp. 381–388.
18. Chinchalkar, S. (2001), "Determination of crack location in beams using natural frequencies", *Journal of Sound and Vibration*, Vol. 247, No. 3, pp. 417–429.
19. Lee, J. (2009), "Identification of multiple cracks in a beam using natural frequencies", *Journal of Sound and Vibration*, Vol. 320, No. 3, pp. 482–490.
20. Zienkiewicz, O.C. and Zhu, J. (1992), "The superconvergent patch recovery and a posteriori error estimates. Part 1: The recovery technique", *International Journal for Numerical Methods in Engineering*, Vol. 33, No. 7, pp. 1331–1364.
21. Zienkiewicz, O.C. and Zhu, J. (1992), "The superconvergent patch recovery and a posteriori error estimates. Part 2: Error estimates and adaptivity", *International Journal for Numerical Methods in Engineering*, Vol. 33, No. 7, pp. 1365–1382.
22. Wiberg, N.E., Bausys, R. and Hager, P. (1999), "Adaptive *h*-version eigenfrequency analysis", *Computers and Structures*, Vol. 71, No. 5, pp. 565–584.

23. Wiberg, N.E., Bausys, R. and Hager, P. (1999), “Improved eigenfrequencies and eigenmodes in free vibration analysis”, *Computers and Structures*, Vol. 73, No. 1–5, pp. 79–89.
24. Wang, Y., Liu, Z., Yang, H. and Zhuang, Z. (2017), “Finite element analysis for wellbore stability of transversely isotropic rock with hydraulic-mechanical-damage coupling”, *Science China Technological Sciences*, Vol. 60, No. 1, pp. 133–145.
25. Wang, Y., Zhuang, Z., Liu, Z., Yang, H. and Li, C. (2017), “Finite element analysis for inclined wellbore stability of transversely isotropic rock with HMCD coupling based on weak plane strength criterion”, *Science China Technological Sciences*, DOI:10.1007/s11431-016-0460-2.
26. Yuan, S., Wang, Y. and Ye, K. (2013), “An adaptive FEM for buckling analysis of non-uniform Bernoulli–Euler members via the element energy projection technique”, *Mathematical Problems in Engineering*, DOI:10.1155/2013/461832.
27. Yuan, S, Wang, Y. and Xu, J. (2014), “New progress in self-adaptive FEMOL analysis of 2D free vibration problems”, *Enginering Mechanics*, Vol. 31, No. 1, pp. 15–22. (In Chinese) DOI:10.6052/ j.issn.1000-4750.2013.05.ST01.
28. Yuan, S., Ye, K., Wang, Y., Kennedy, D. and Williams, F.W. (2017), Adaptive finite element method for eigensolutions of regular second and fourth order Sturm-Liouville problems via the element energy [J]. *Engineering Computations*. (Accepted)
29. Dimarogonas, A.D. (1996), “Vibration of cracked structures: a state of the art review”, *Engineering Fracture Mechanics*, Vol. 55, No. 5, pp. 831–857.
30. Moezi, S.A., Zakeri, E., Zare, A. and Nedaeib, M. (2015), “On the application of modified cuckoo optimization algorithm to the crack detection problem of cantilever Euler–Bernoulli beam”, *Computers and Structures*, Vol. 157, pp. 42–50.
31. Guan, H. and Karbhari, K.M. (2008), “Improved damage detection method based on element modal strain damage index using sparse measurement”, *Journal of Sound and Vibration*, Vol. 309, No. 3, pp. 465–494.
32. Owolabi, G.M., Swamidas, A.S.J. and Seshadri, R. (2003), “Crack detection in beams using changes in frequencies and amplitudes of frequency response functions”, *Journal of Sound and Vibration*, Vol. 265, No. 1, pp. 1–22.
33. Maghsoodi, A., Ghadami, A. and Mirdamadi, H.R. (2013), “Multiple-crack damage detection in multi-step beams by a novel local flexibility-based damage index”, *Journal of Sound and*

Vibration, Vol. 332, No. 2, pp. 294–305.

34. Al-Said, S.M. (2007), "Crack identification in a stepped beam carrying a rigid disk", *Journal of Sound and Vibration*, Vol. 300, No. 3, pp. 863–876.
35. Al-Said, S.M. (2008), "Crack detection in stepped beam carrying slowly moving mass", *Journal of Sound and Vibration*, Vol. 14, No. 12, pp. 1903–1920.
36. Morassi, A. (2001), "Identification of a crack in a rod based on changes in a pair of natural frequencies", *Journal of Sound and Vibration*, Vol. 242, No. 4, pp. 577–596.
37. Lele, S.P. and Maiti, S.K. (2002), "Modelling of transverse vibration of short beams for cracks detection and measurement of crack extension", *Journal of Sound and Vibration*, Vol. 257, No. 3, pp. 559–583.
38. Nikolakopoulos, P. G., Katsareas, D. E. and Papadopoulos, C. A. (1997), "Crack identification in frame structures", *Computers and Structures*, Vol. 64, No. 1–4, pp. 389–406.
39. Narkis, Y. (1994), "Identification of crack location in vibrating simply supported beams", *Journal of Sound and Vibration*, Vol. 172, No. 4, pp. 549–558.
40. Dado, M. H. (1997), "A comprehensive crack identification algorithm for beam under different end conditions", *Applied Acoustics*, Vol. 51, No. 4, pp. 381–398.
41. Hu, J. and Liang, R.Y. (1993), "An integrated approach to detection of cracks using vibration characteristics", *Journal of the Franklin Institute*, Vol. 330, No. 5, pp. 841–853.
42. Patil, D.P. and Maiti, S.K. (2003), "Detection of multiple cracks using frequency measurements", *Engineering Fracture Mechanics*, Vol. 70, No. 12, pp. 1553–1572.
43. Ruotolo, R. and Surace, C. (1997), "Damage assessment of multiple cracked beams: numerical results and experimental validation", *Journal of Sound and Vibration*, Vol. 206, No. 4, pp. 567–588.
44. Shifrin, E.I. and Ruotolo, R. (1999), "Natural frequencies of a beam with an arbitrary number of cracks", *Journal of Sound and Vibration*, Vol. 222, No. 3, pp. 409–423.
45. Labib, A., Kennedy, D. and Featherston, C.A. (2015), "Crack localisation in frames using natural frequency degradations", *Computers and Structures*, Vol. 157, pp. 51–59.
46. Zienkiewicz, O.C. and Taylor, R.L. (2000), *The Finite Element Method*, fifth ed., Butterworth– Heinemann, Oxford.
47. Clough, R.W. and Penzien, J. (1993), *Dynamics of Structures*, second ed., McGraw-Hill, New York.